表5 マウス腎臓に存在する主な糖鎖の糖組成及び推定構造

Sugar No.	Composition[a]	Deduced structure	Lewis type
a	$dHex_3Hex_5HexNAc_5$	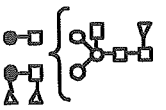	Le^y
b	$dHex_2Hex_5HexNAc_5$	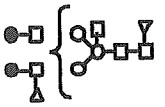	Le^x
c	$Hex_8HexNAc_2$	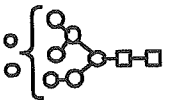	
d	$Hex_9HexNAc_2$	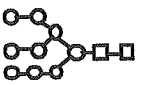	
e	$dHexHex_4HexNAc_5$	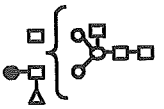	Le^x
f	$dHex_3Hex_5HexNAc_5$	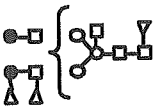	Le^y
g	$Hex_6HexNAc_2$	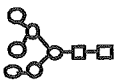	
h	$dHex_2Hex_4HexNAc_5$	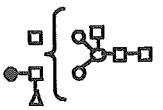	Le^x
I	$Hex_7HexNAc_2$		
j	$Hex_5HexNAc_2$	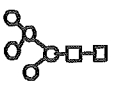	

[a] dHex, deoxyhexose; Hex, hexose; HexNAc, *N*-acetylhexosamine
△, Fuc; ●, Gal; ○, Man; □, GlcNAc

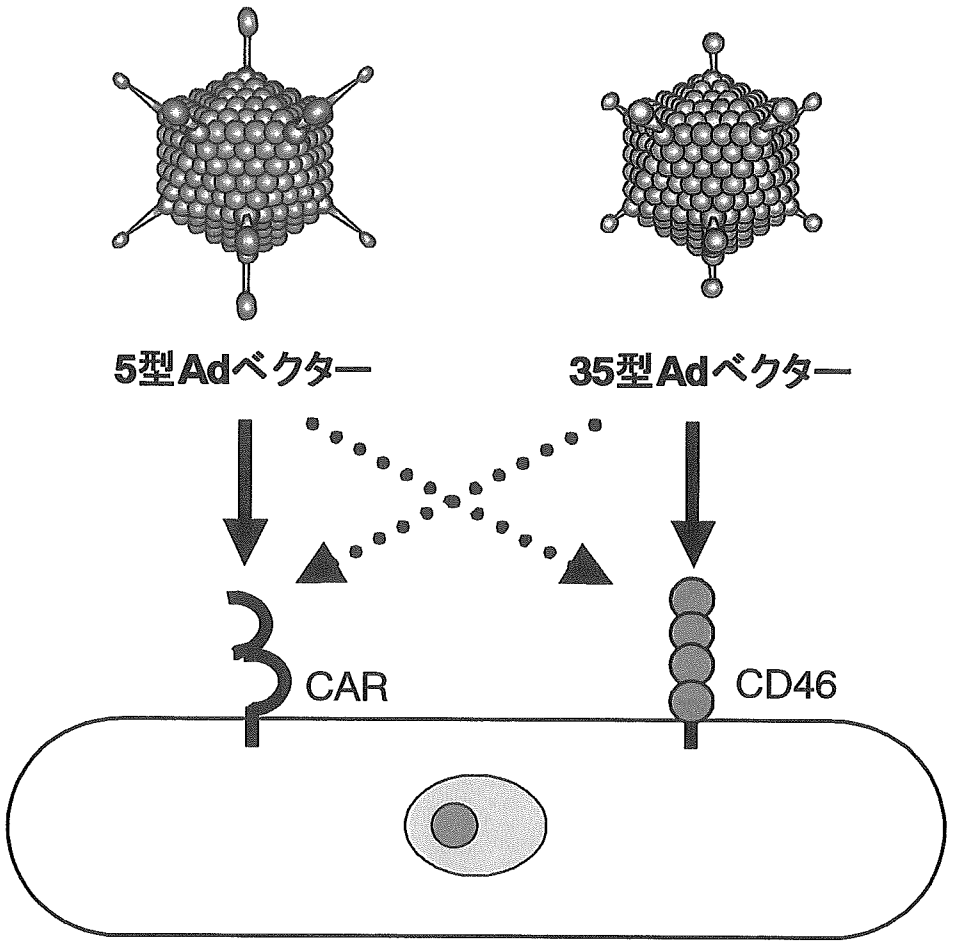

図35　　Diagram of interaction between Ad vectors and receptors. Ad serotype 5 vectors (subgroup C) utilize coxsakievirus and adenovirus receptor (CAR) for infection, while Ad serotype 35 vectors (subgroup B) utilize human CD46 for infection.

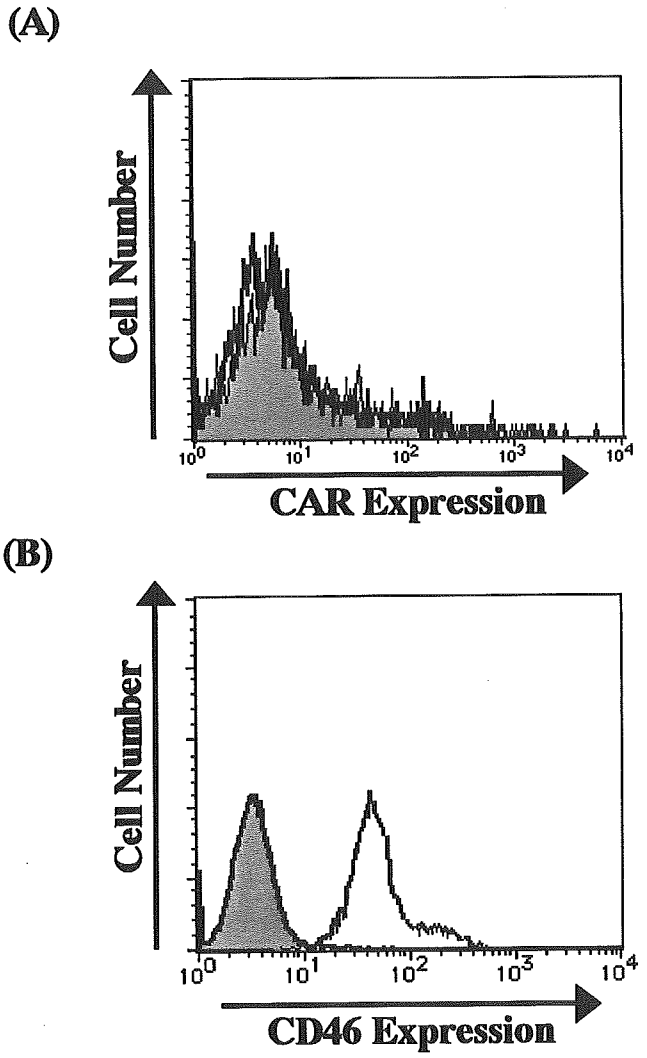

図36　　Expression of Ad receptors on human bone-marrow CD34⁺ cells. (A) Coxsachievirus and adenovirus receptor (CAR) (a receptor for Ad5), (B) CD46 (a receptor for Ad35). Human bone-marrow CD34+ cells were incubated with FITC-conjugated anti-CD46 antibody for measurement of CD46. For analysis of CAR expression, the cells were treated anti-CAR antibody. After a 1-hr incubation, cells were washed and resuspended in a staining buffer containing phycoerythrin (PE)-labeled anti-mouse IgG antibody. After a 1-hr incubation, the cells were subjected to flowcytomteric analysis. As a negative control, the cells were incubated with an irrelevant antibody (shaded histogram).

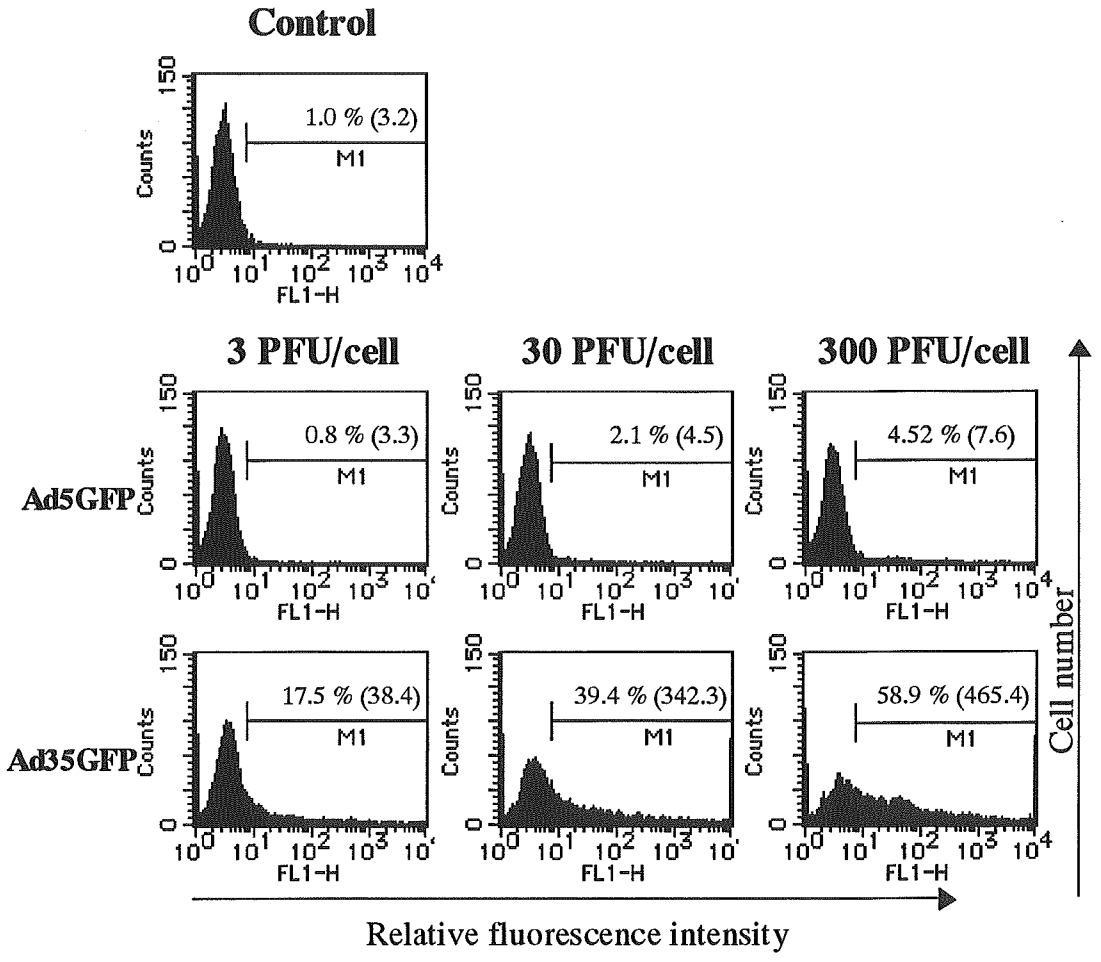

図37　GFP expression in human bone-marrow CD34⁺ cells transduced with Ad5GFP and Ad35GFP. Human CD34⁺ cells were suspended in the medium containing the cytokine cocktail (3 x 10^5 cells/ml). The cells were seeded into a 96-well plate (1 x 10^4 cells/well), and equal volumes of the Ad vectors were applied to the cells 16-18 hrs after seeding. Forty-eight hour later, GFP expression in the cells were measured by flow cytometry.

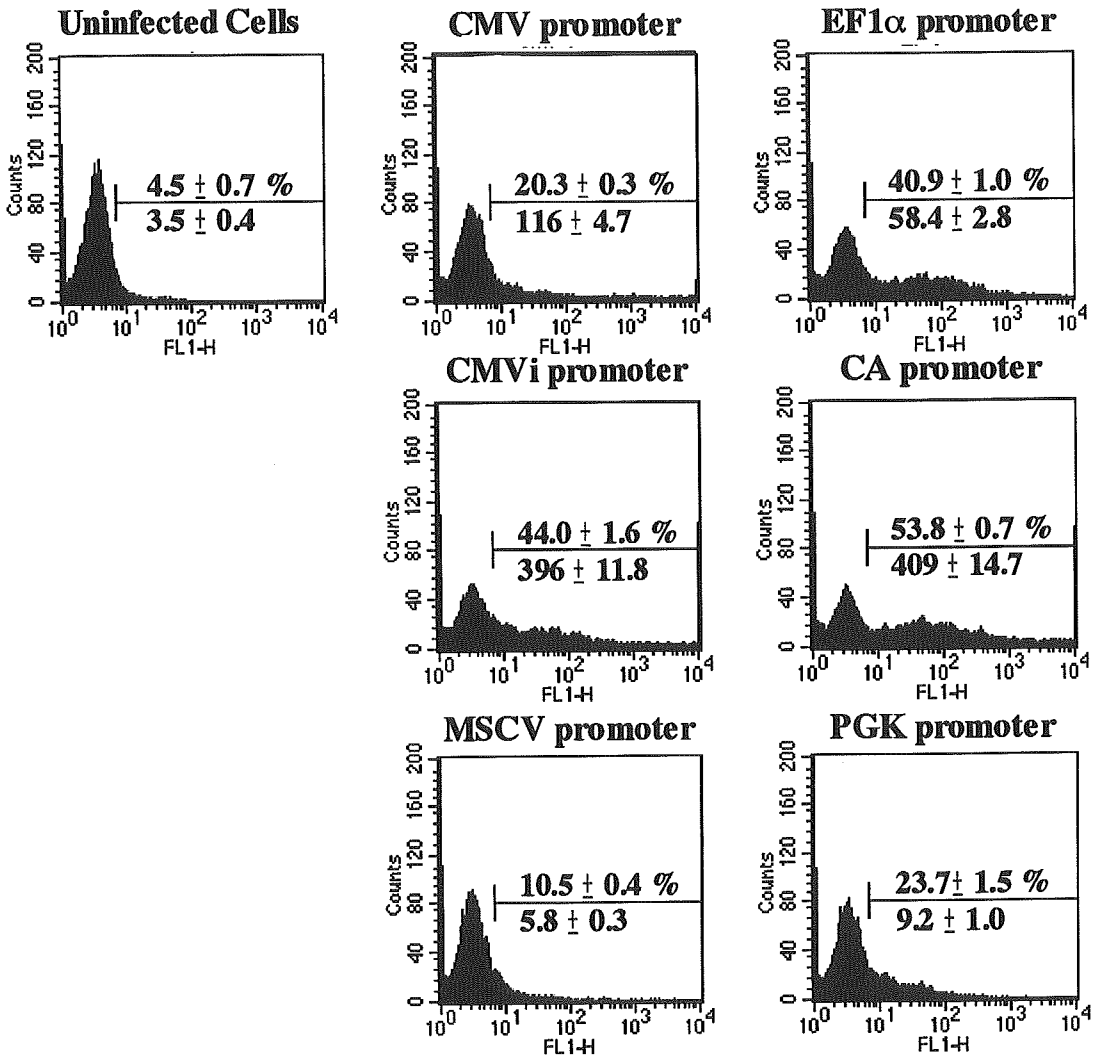

図38　　Comparison of promoter activities in human bone-marrow CD34⁺ cells transduced with Ad35 vectors. The CD34⁺ cells were transduced with Ad35 vectors at 6000 VP/cell for 6 hrs, washed, and resuspended in medium. Forty-eight hours later, GFP expression was measured by flow cytometry. The results are shown as a percentage of GFP-positive cells (upper) and the mean fluorescenceintensity (MFI) (lower) in the panel. All data represent the means ± S.D. of three experiments.

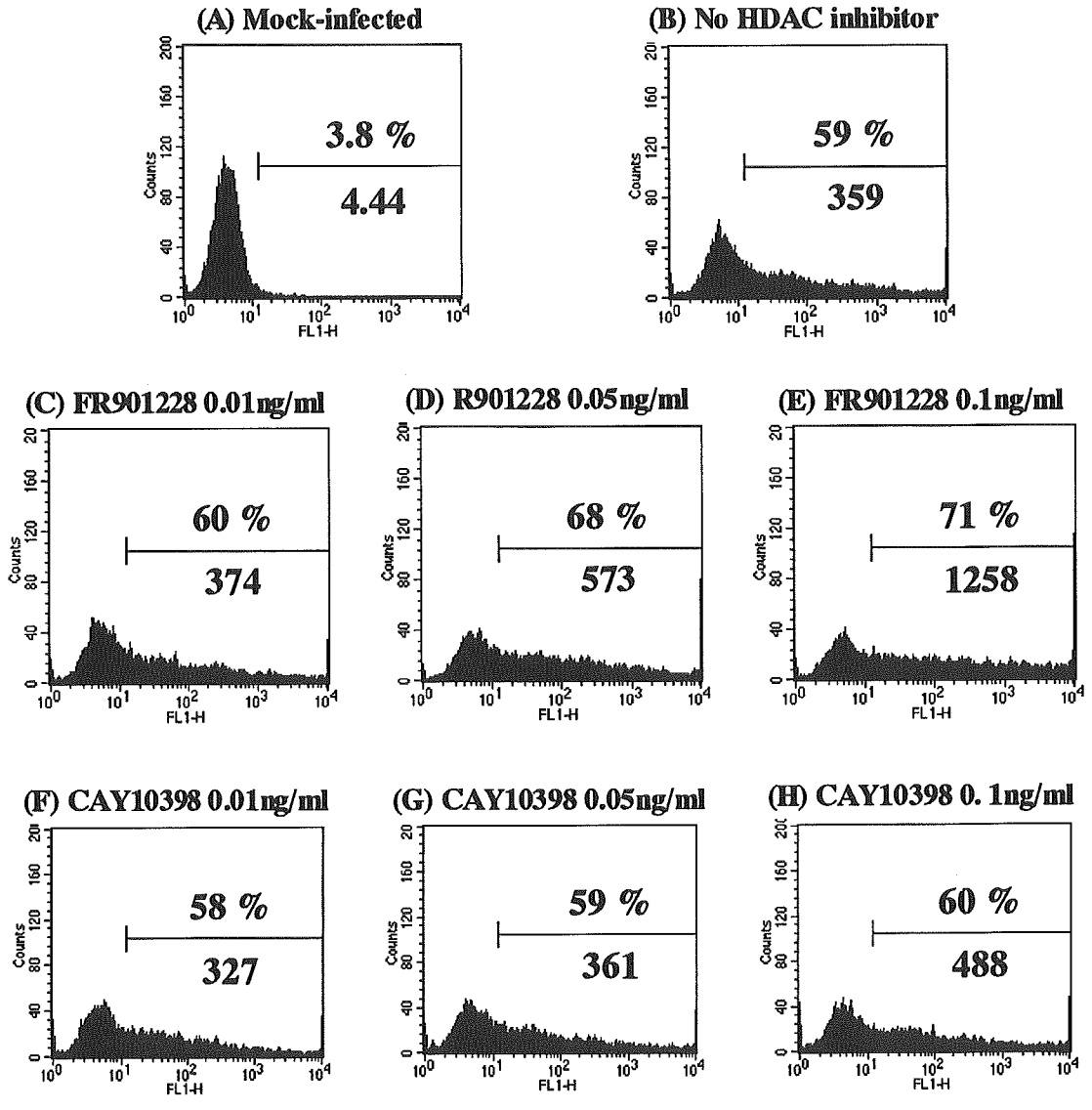

図39 Effect of treatment with HDAC inhibitors on the transduction of human bone-marrow CD34⁺ cells. The CD34⁺ cells were incubated with HDAC inhibitors at the indicated concentrations and Ad35 vectors at 6000 VP/cell for 6 hrs, washed, and resuspended in medium. Forty-eight hours later, GFP expression was measured by flow cytometry. The results are shown as a percentage of GFP-positive cells (upper) and the mean fluorescence intensity (MFI) (lower) in the panel.

図40　臍帯血からのOECの光顕像

OEC-1

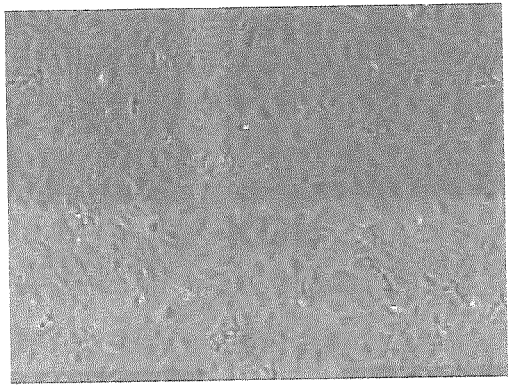

OEC-2

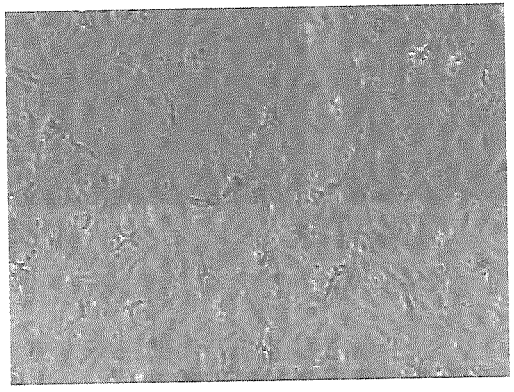

OEC-3

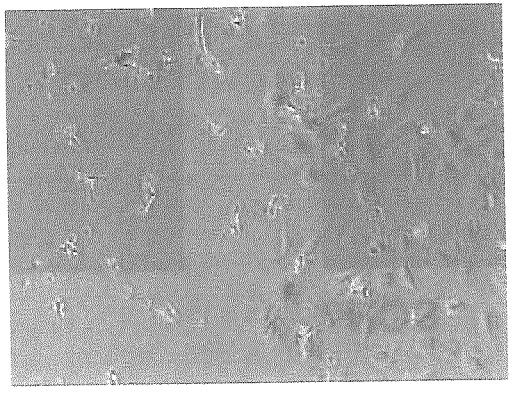

OEC-4

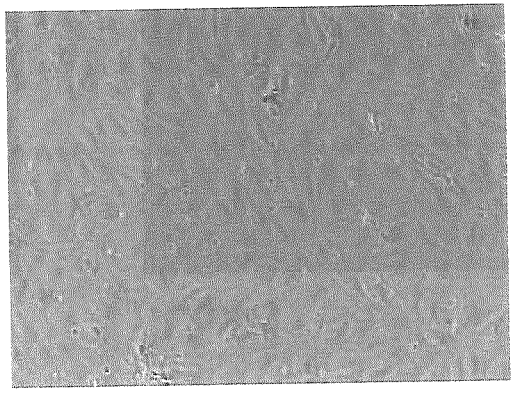

図41　臍帯血OECが血管内皮細胞である同定

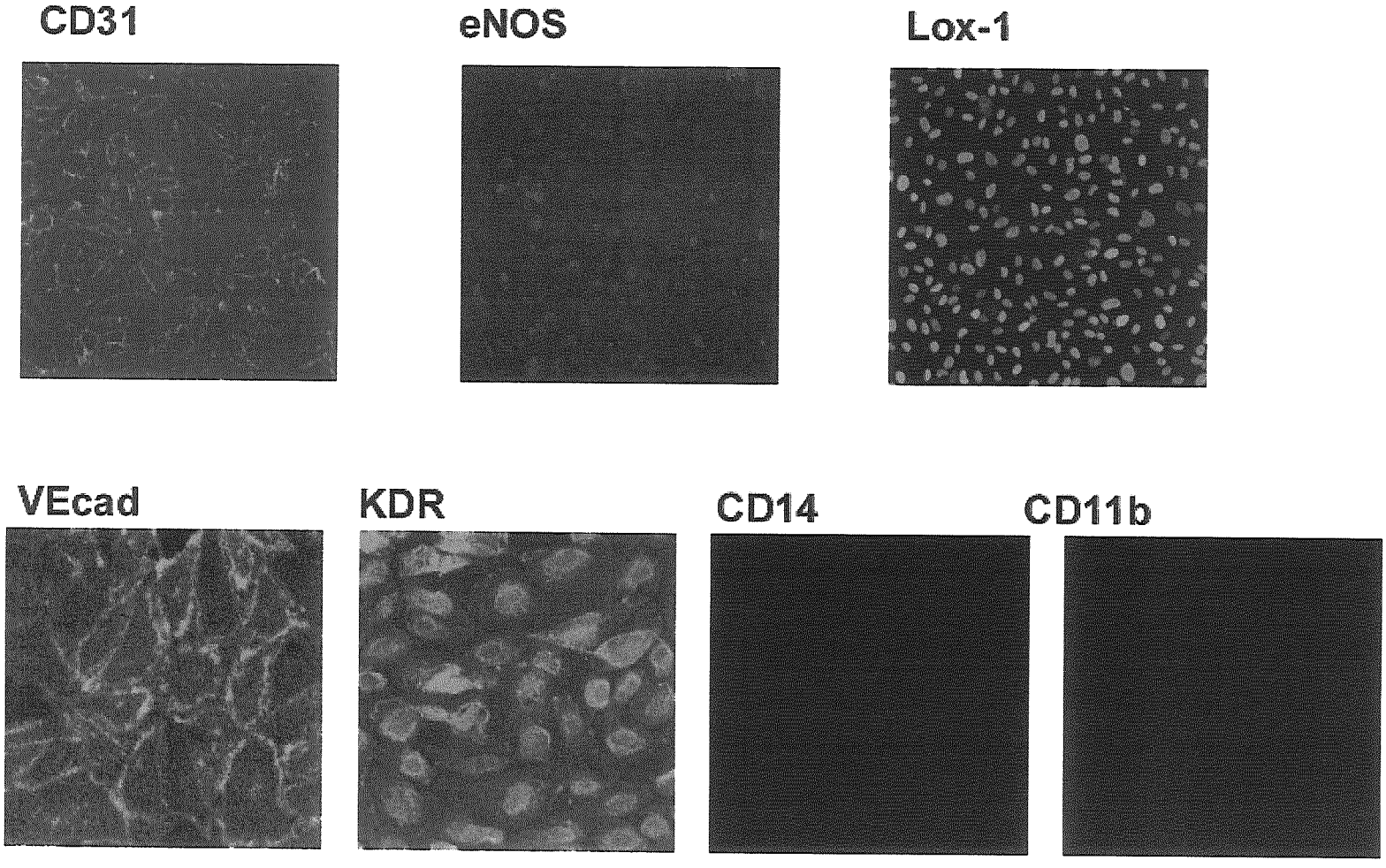

図42　臍帯血OECが血管内皮細胞である同定

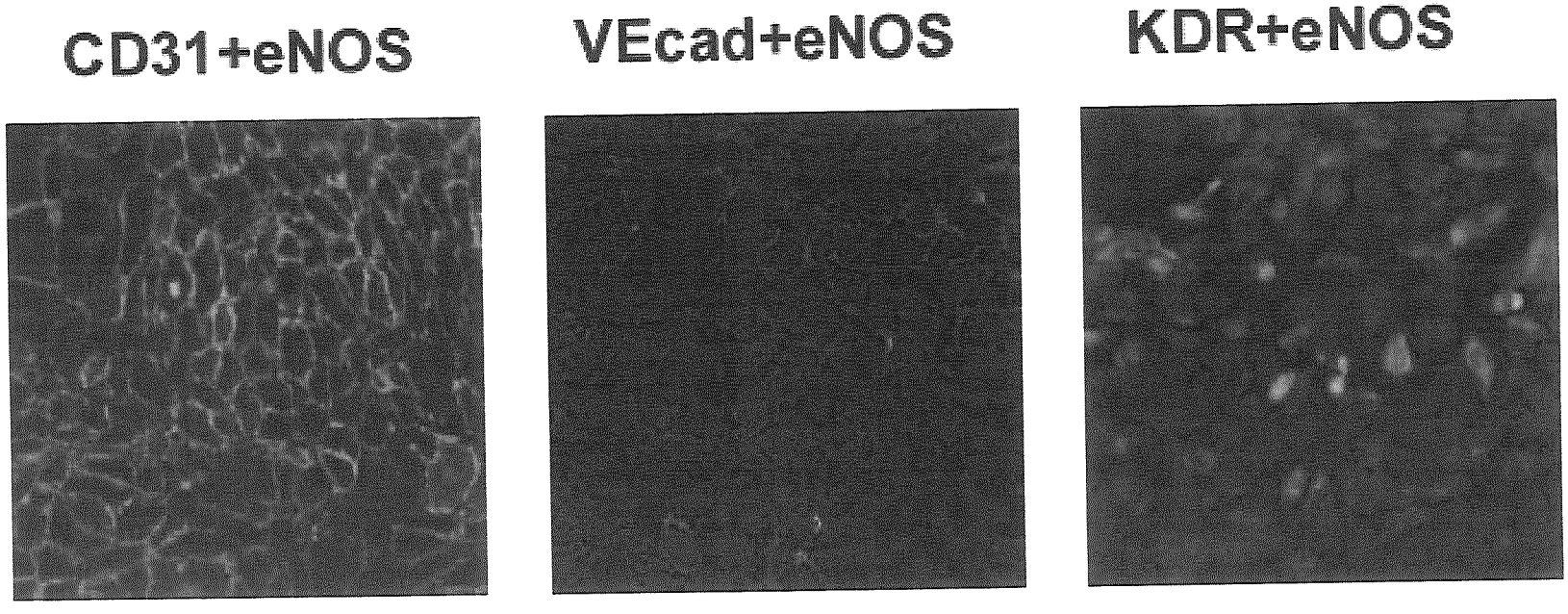

図43　臍帯血OECの管腔形成能

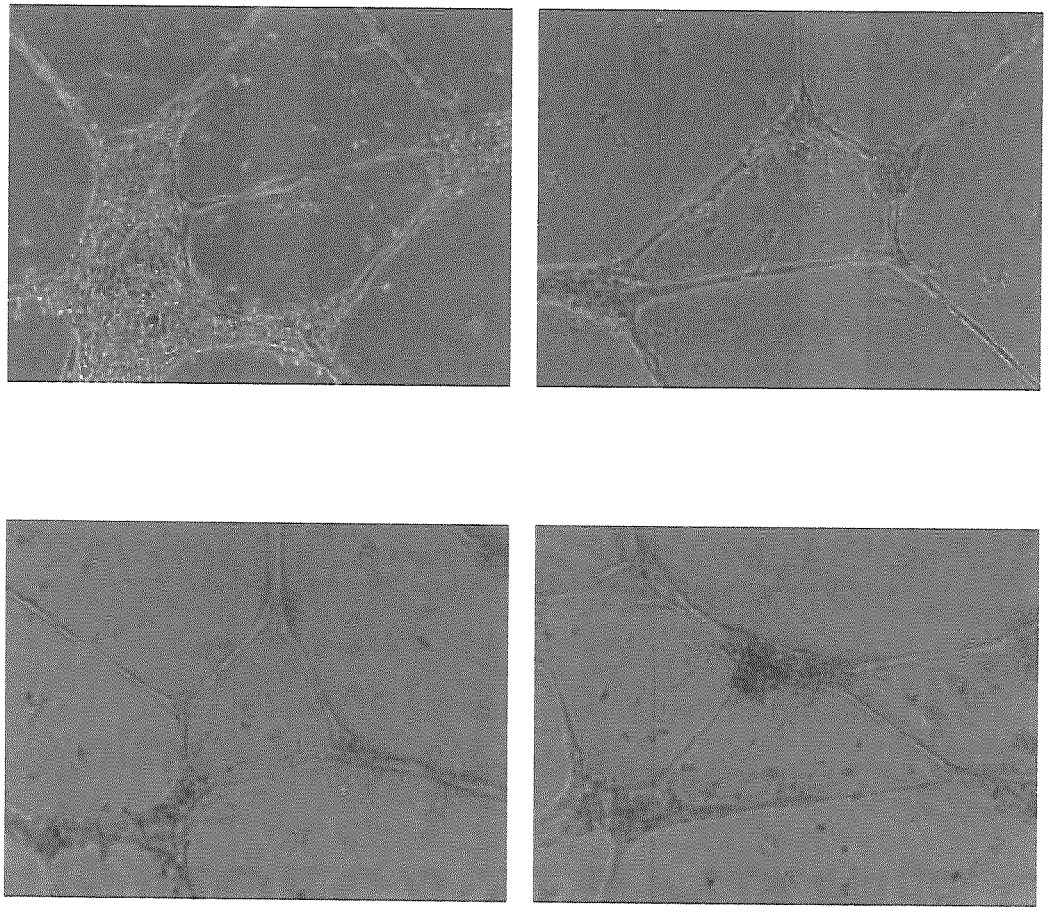

図44　臍帯血OECを培養する際、混入する血管平滑筋細胞の同定

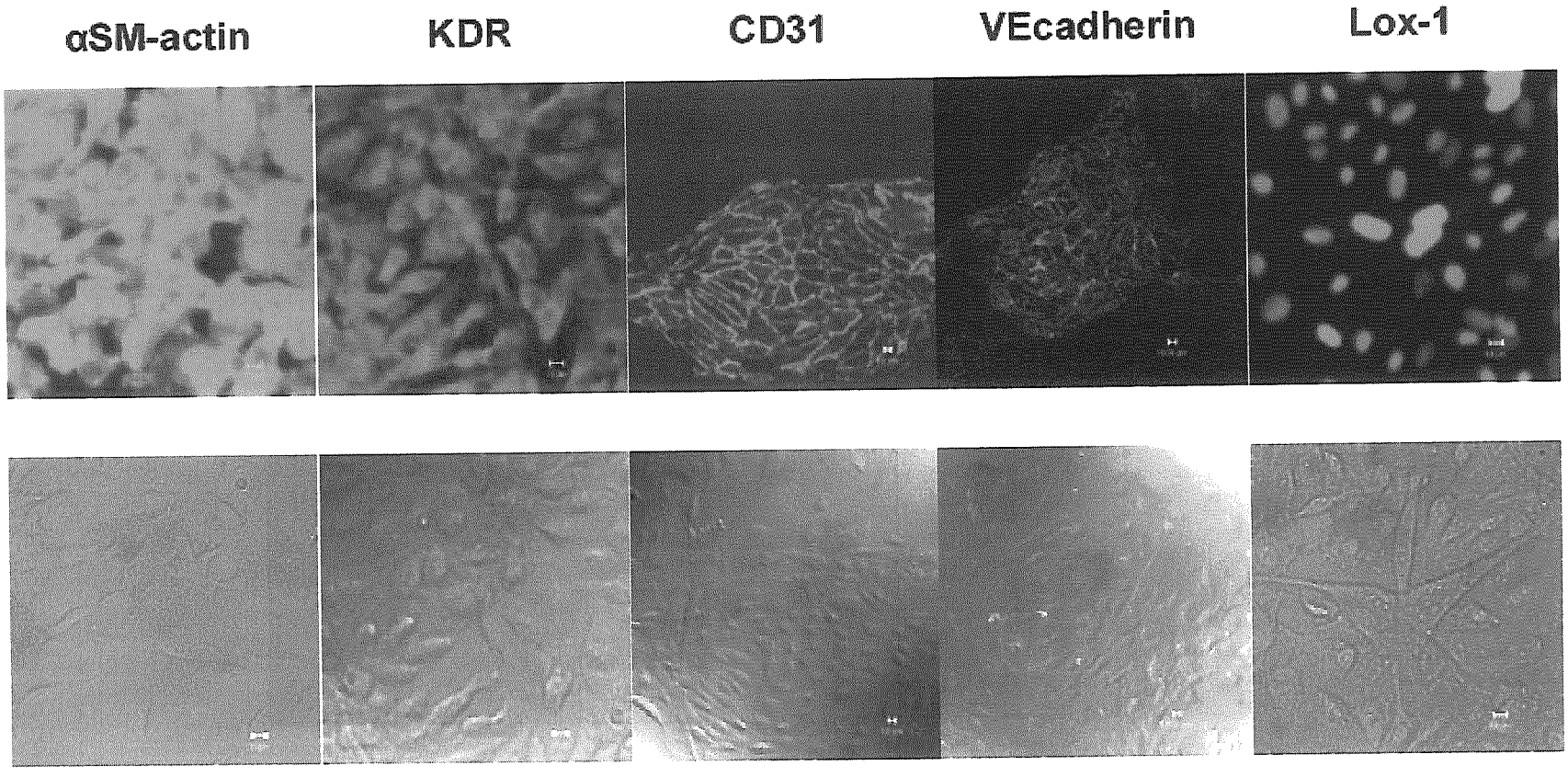

図45　末梢血OECが形成するコロニー

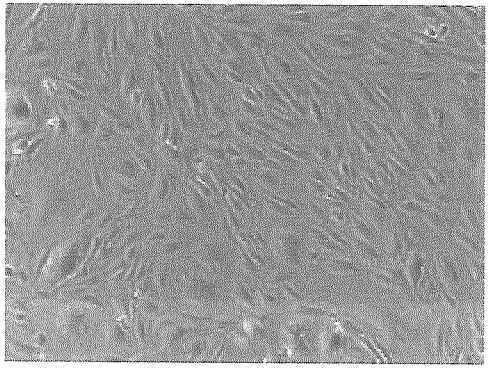

1-Colony-22d-2

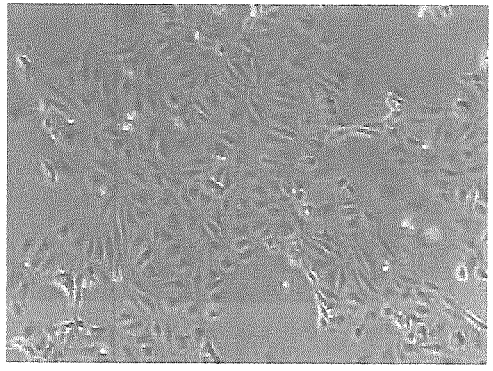

2-Colony-22d-1

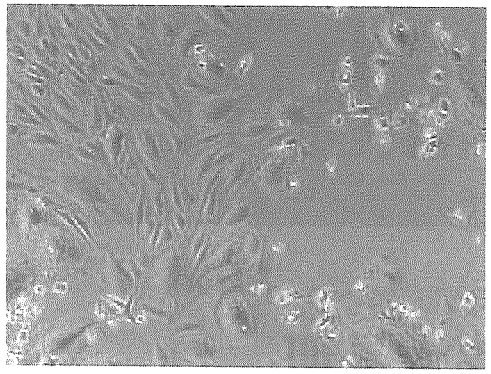

1-Colony-22d-2

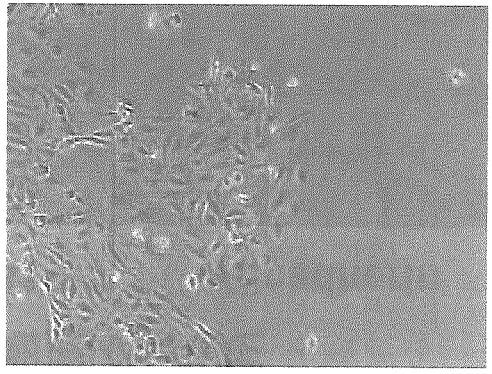

2-Colony-22d-2

図46　末梢血OECが血管内皮細胞である同定

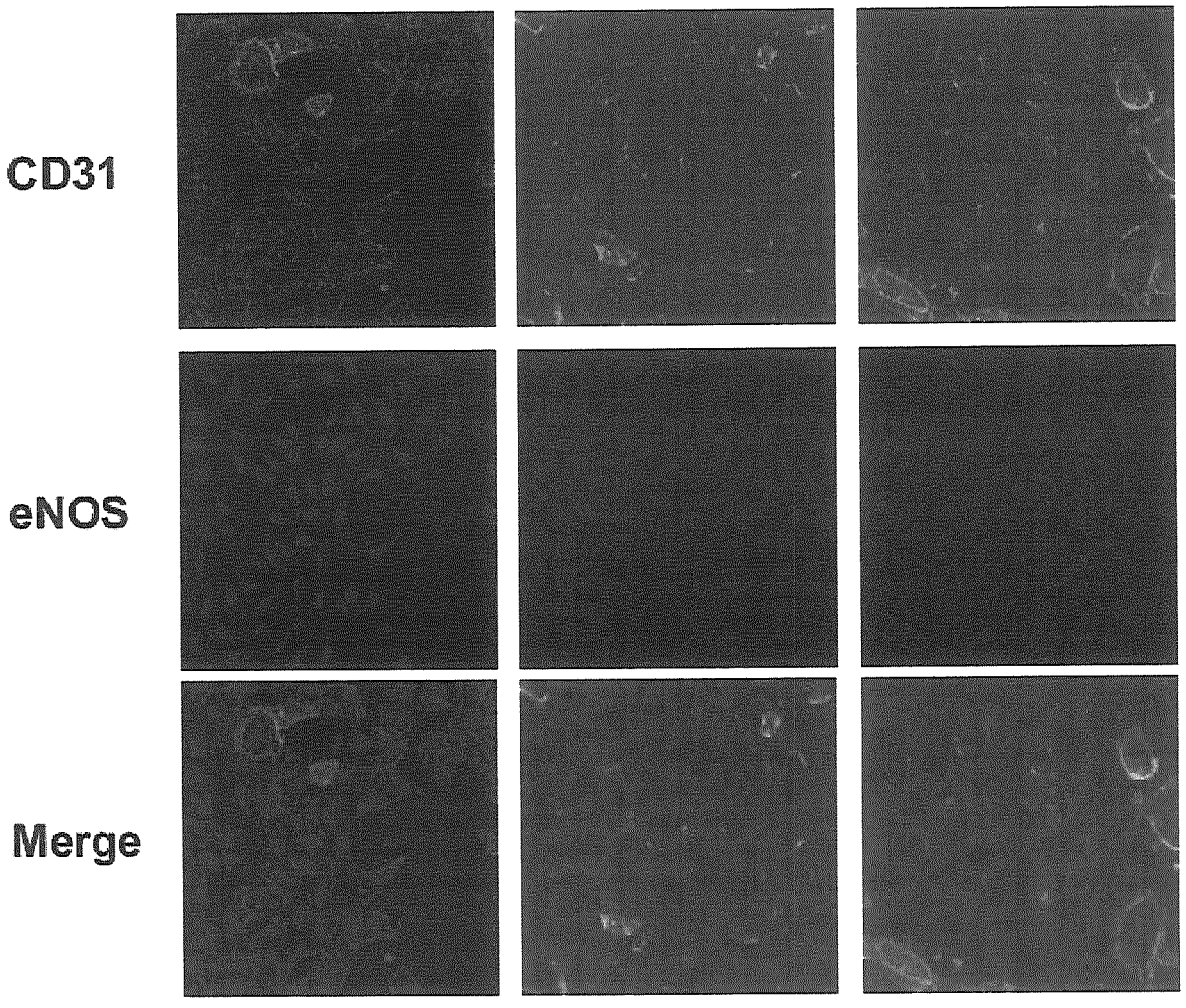

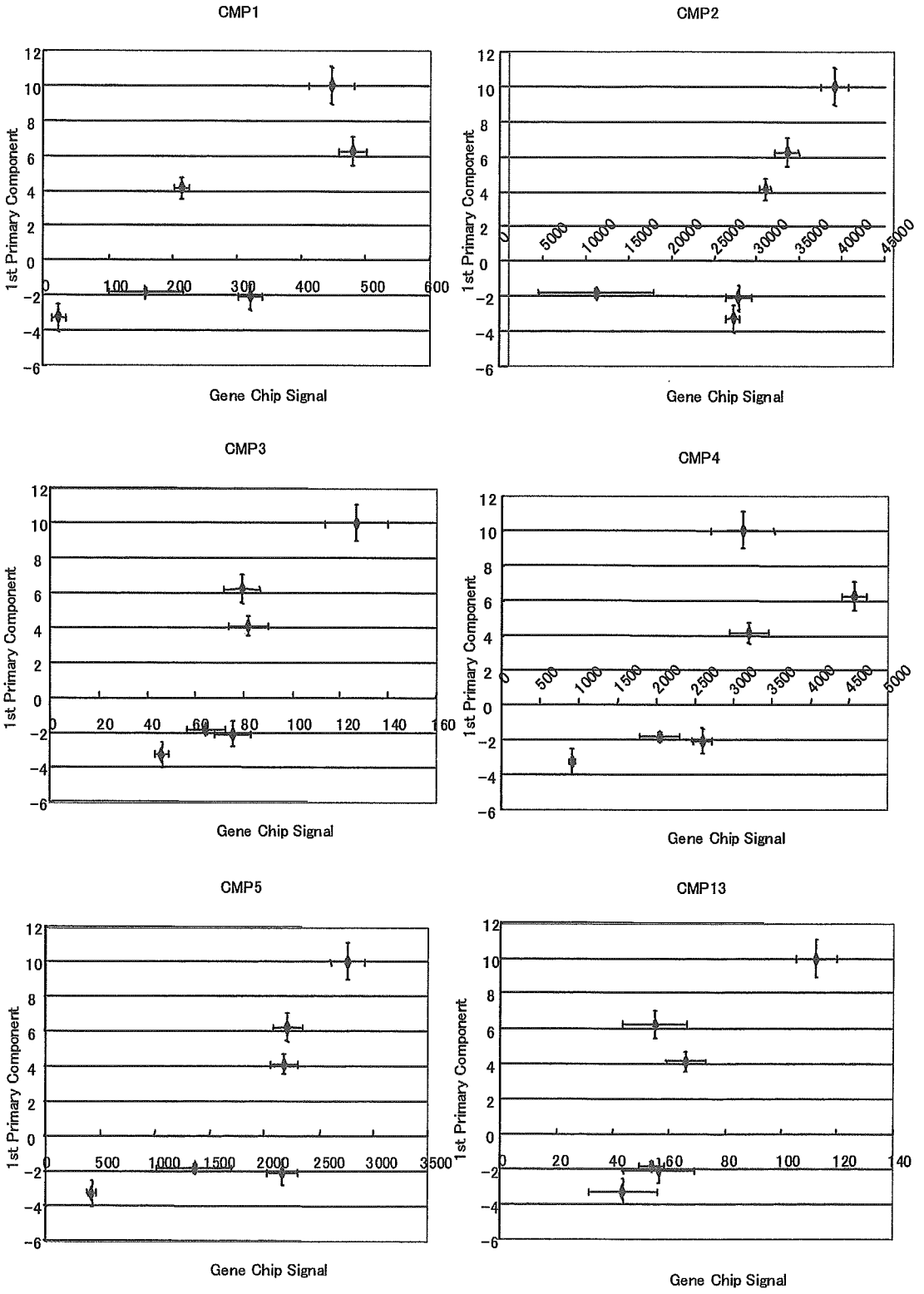

図47 CMP遺伝子の発現と細胞株の心筋分化傾向の相関
[各細胞株の平均値±S.E.M. (n=5-6)]

蛍光像(BLOCK-iT
＝蛍光StealthRNAi)

位相差像

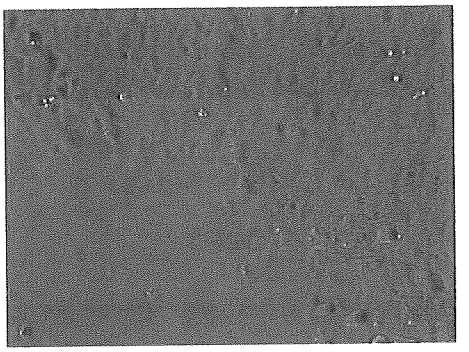

重ね合わせ

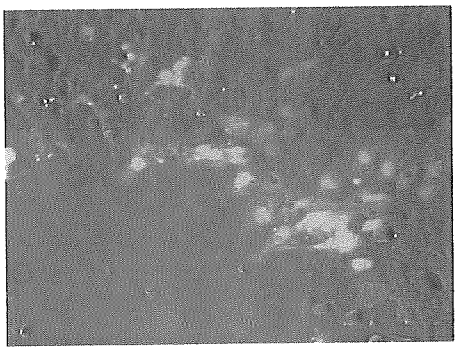

図48 CL6G52細胞へのStealth RNAiのトランスフェクション

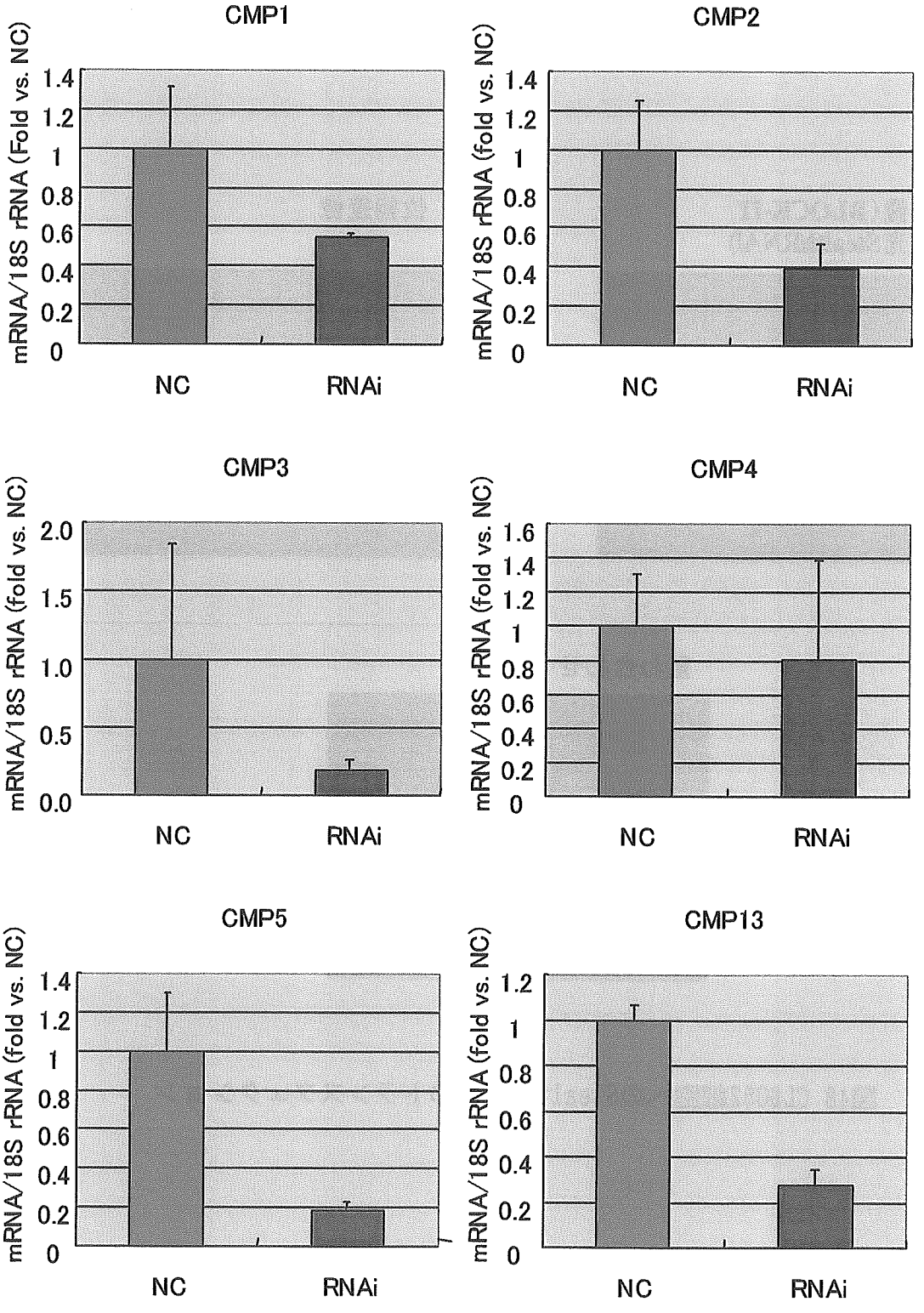

図49 CL6G52細胞におけるCMP遺伝子の発現に対するRNAi
[平均値±S.E.M. (n=3)]

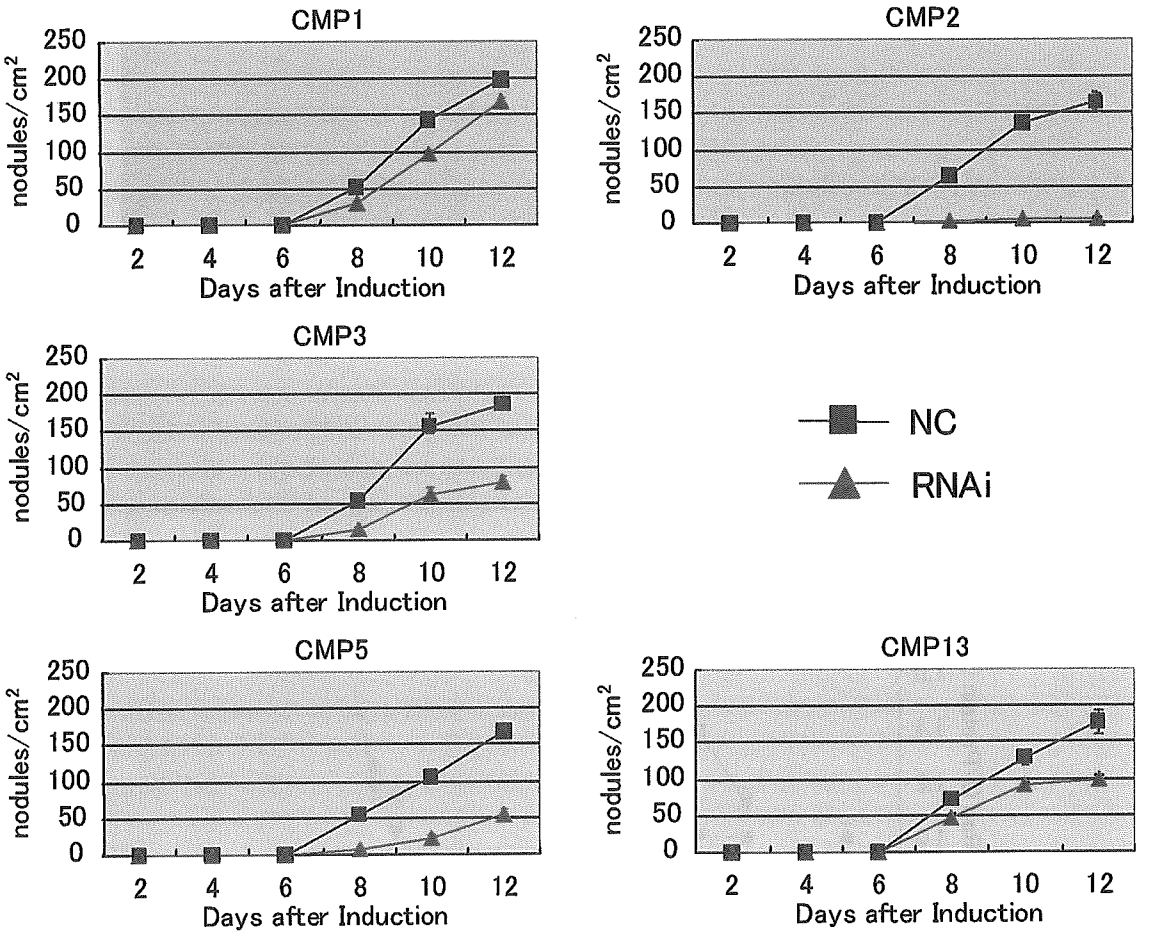

図50 CL6G52細胞の心筋細胞分化に対するCMP遺伝子発現のRNAi の効果
[平均値±S.E.M. (n=4)]

A

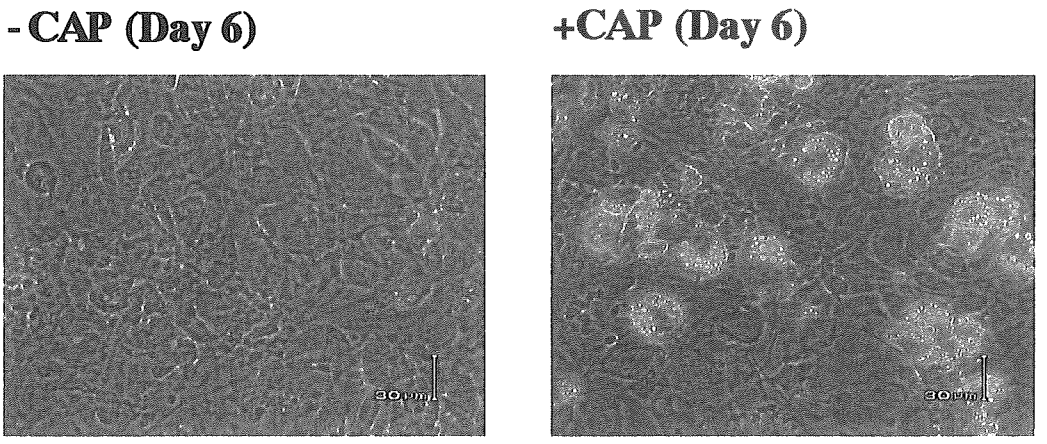

B

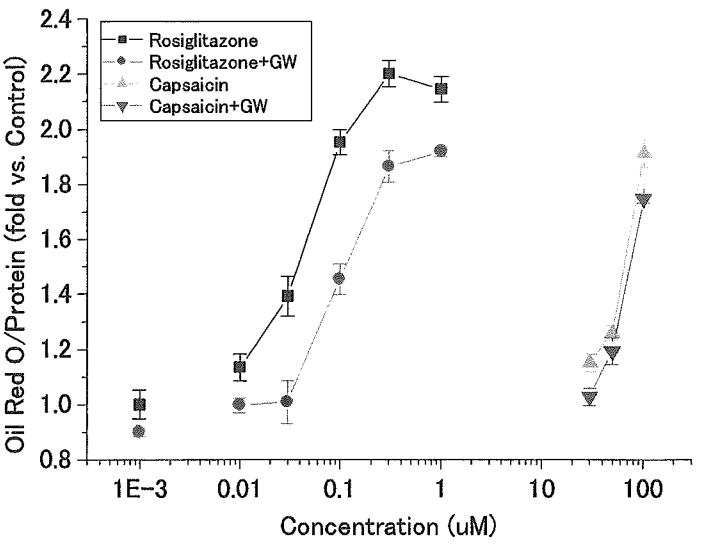

図51 カプサイシンの脂肪細胞誘導作用
6日間のカプサイシン処理(100mM)により脂肪細胞に分化した10T1/2細胞 (A)
10T1/2細胞をOilRed O染色した後に定量 (B)
データは平均値±S.E.M. (n=3)で示す。

	Oil Red O/Protein (fold vs. NC)
NC(DMSO)	1.000 ±0.047
CAP(30 μ M)	5.018 ±0.127
CAP(100 μ M)	10.462 ±0.509
CAP(100 μ M)+CPZ(10 μ M)	3.527 ±0.036
CAP(100 μ M)+RR(10 μ M)	6.340 ±0.313

表6 カプサイシンの脂肪細胞誘導作用に対する TRPV阻害薬の効果
10T1/2細胞におけるカプサイシン(CAP)処理による脂肪細胞分化に対する
カプサゼピン(CPZ)およびルテニウムレッド(RR)の効果
データは平均値± S.E.M.(n=4)で示す。

A.	Oil Red O/Protein (fold vs. NC)
NC(DMSO)	1.000 ± 0.027
l-Menthol (100 μ M)	1.285 ± 0.076
Icilin (0.1 μ M)	1.426 ± 0.061

B.	Oil Red O/Protein (fold vs. NC)
NC(DMSO)	1.000 ± 0.027
Allyl isothiocyanate (10 μ M)	2.177 ± 0.118
t-Cinnamaldehyde (30 μ M)	2.838 ± 0.158
Icilin (0.1 μ M)	1.426 ± 0.061

表7 TRPM8およびTRPA1に対するアゴニストの脂肪細胞誘導作用
TRPM8 アゴニスト(A)およびTRPA1アゴニスト(B)の10T1/2細胞における
脂肪細胞分化誘導作用
データは平均値± S.E.M.(n=4)で示す。

表8　Fibronectin and recombinant cell adhesive proteins used in this study

Proteins	Structure	Molecular Weight
Fibronectin	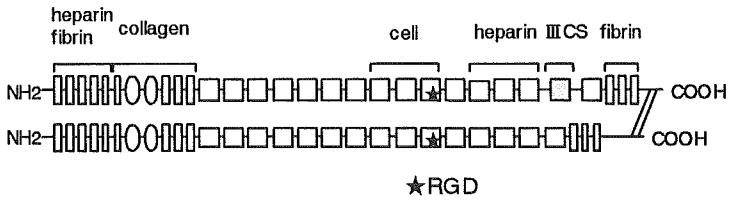	230K x 2
ProNectin F	Head-[(GAGAGS)9GAAVTGRGDSPASAAGY]12-Tail ★	73K
ProNectin F Plus	Positively charged, water-soluble variant of Pronectin F	73K
ProNectin L	Head-[(GAGAGS)9GAAPGASIKVAVSAGPSAGY]12-Tail ◆	76K
RetroNectin	Chimeric peptide of human fibronectin fragment 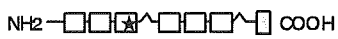	63K
Attachin	A fusion protein constructed by molecular biotechnology	30K

Fibronectin

[] Type I module

() Type II module

□ Type III module

★: cell attachment sequence derived from fibronectin

◆: cell attachment sequence derived from laminin